

# Landau-Zener-Stückelberg Interference of Microwave Dressed States of a Superconducting Phase Qubit

Guozhu Sun<sup>1,2,3\*</sup>, Xueda Wen<sup>3</sup>, Bo Mao<sup>2</sup>, Yang Yu<sup>3</sup>, Jian Chen<sup>1,3</sup>, Weiwei Xu<sup>1,3</sup>, Lin Kang<sup>1,3</sup>,  
Peiheng Wu<sup>1,3</sup>, Siyuan Han<sup>1,2\*</sup>

<sup>1</sup>*Research Institute of Superconductor Electronics, School of Electronic Science and Engineering, Nanjing University, Nanjing 210093, China*

<sup>2</sup>*Department of Physics and Astronomy, University of Kansas, Lawrence, KS 66045, USA*

<sup>3</sup>*National Laboratory of Solid State Microstructures, School of Physics, Nanjing University, Nanjing 210093, China*

**Dressed state<sup>1</sup>, the eignstate of a combined system of light and matter, has been proposed as fundamental concept to interpret quantum interaction between photons and atoms or molecules. Recently, this picture has been extended to describe the hybrid system of photons and superconducting circuits<sup>2-4</sup>. Here, we present the first observation of Landau-Zener-Stückelberg (LZS) interference<sup>5</sup> of the dressed states arising from an artificial atom, a superconducting phase qubit<sup>6</sup>, interacting with a microwave field. The LZS interference fringes, which depend on the sweep rate, the frequency and power of the microwave, and the initial state of the qubit, agree with the theoretical prediction quantitatively. The LZS interference between the microwave dressed qubit states also enables us to control the quantum states of a tetrapartite solid-state system with ease and precision, demonstrating the feasibility of**

**implementing efficient multipartite quantum logic gates with this unique approach.**

One of those remarkable features in the quantum systems is the energy level quantization. The energy level diagram of simple quantum systems, such as atoms and nuclear spins, may exhibit avoided level crossings as a function of an external control parameter, as shown in the inset of Fig. 1c. If one adjusts the external control parameter to sweep the system across one of the avoided level crossings back and forth, the quantum states evolving along the two different pathes will interfere, generating the well-known Landau-Zener-Stückelberg (LZS) interference. LZS interference was originally observed in helium Rydberg atoms by Yoakum et al<sup>7</sup>. Recent progresses in solid-state qubits have stimulated strong interests in LZS interference in superconducting qubits<sup>5, 8–15</sup> and electron spins<sup>16</sup>. However, most of the previous works were performed in simple systems having avoided level crossings in their energy diagrams. Since monochromatic electromagnetic fields have been extensively used to control quantum states, from both theoretical curiosity and practical significance it is interesting and important to know whether LZS interference can be realized and observed between the dressed states, generated from the interaction between photons and atoms or even macroscopic quantum objects such as superconducting qubits<sup>17–19</sup>. The concept of dressed states describes very well the behavior of the combined systems of photons and atoms<sup>1</sup>. Recently the dressed state picture has been applied to treat intriguing phenomena arising from interaction between photons and superconducting circuits, opening a new field named circuit quantum electrodynamics (C-QED)<sup>2–4</sup>. Although creating avoided crossings with dressed states of a Cooper pair box has been proposed<sup>10, 20</sup>, no evidence of LZS interference has been reported so far. In this work, we report the first observation of LZS interference of the microwave dressed

states of a superconducting phase qubit (SPQ) by applying nanosecond dc triangle pulses to sweep the system across the avoided crossing between the microwave dressed qubit states. We show that the observed oscillations in the SPQ's occupational probability are the result of LZS interference. Furthermore, we developed a theoretical model based on the microwave dressed states that quantitatively reproduced the dependence of LZS interference fringes on the sweep rate, the microwave power, the microwave frequency, and the initial state of the qubit. Since these external parameters can be controlled precisely in experiments, LZS interference of the microwave dressed states may provide a new approach to improve the speed and fidelity of quantum information processing.

One form of the SPQ is based on the rf-SQUID, which consists of a superconducting loop interrupted by a Josephson junction as shown in Fig. 1a. The superconducting phase difference  $\varphi$  across the junction serves as this macroscopic quantum object's dynamic variable. Such a "phase particle" has a discrete eigenenergy spectrum which is a function of the external flux bias. When properly biased, the ground and the first excited states in one of the potential wells act as  $|0\rangle$  and  $|1\rangle$  of the qubit<sup>6</sup>, respectively. Fig. 1c shows the measured spectroscopy of the SPQ used in the experiment. Setting  $\hbar = 1$ , the level spacing between  $|1\rangle$  and  $|0\rangle$ ,  $\omega_{10} = \omega_1 - \omega_0$ , decreases with the external flux bias due to the anharmonicity of the potential well. Ideally, one expects that  $\omega_{10}$  would be a continuous function of the flux bias. However, three avoided crossings, near 16.45 GHz, 16.21 GHz, and 16.10 GHz, resulting from couplings between the qubit and microscopic two-level systems (TLSs)<sup>6,21</sup> were observed. Although the microscopic origin of TLSs and the mechanism of their interaction with superconducting qubits are still unclear and difficult to control, their quantum nature has been explored for quantum information applications such as quantum memory<sup>22</sup> and

qubit<sup>15,23</sup>.

The experimental procedure to realize and observe LZS interference between microwave dressed qubit states is depicted in Fig. 1b. The qubit initialized in  $|0\rangle$  and dc biased at  $\Phi_i$ . Then a microwave pulse of width  $t_{mw}$  was applied, which generated a set of dressed states. The microwave frequency  $\omega$  was chosen to be greater than  $\omega_{10}$  at  $\Phi_i$ . The intersecting of the dressed states  $|0, n+1\rangle$  and  $|1, n\rangle$  produced an avoided crossing. At the same time, a concurrent dc triangle pulse of width  $t_\Lambda = t_{mw}$  was applied to sweep the system's instantaneous flux bias from  $\Phi_i$  to  $\Phi_{LZS}$  and then back to  $\Phi_i$ . After turning off the triangle pulse, the population of the qubit state  $|1\rangle$ ,  $P_1$ , was measured. Then we repeated the above process with different values of  $\Phi_{LZS}$  and  $t_\Lambda$  to obtain a plot of  $P_1$  versus  $\Phi_{LZS}$  and  $t_\Lambda$  as shown in Fig. 2a. Note that in Fig. 2 and Fig. 3,  $\Phi_{LZS}$  is measured with respect to  $\Phi_i$ . For  $\Phi_{LZS} < \Phi_r$ , where the applied microwave was resonant with  $\omega_{10}$ , the system could not reach the avoided crossing, and thus there was no Landau-Zener (LZ) transition and LZS interference. The qubit could only be excited directly to  $|1\rangle$  by Rabi oscillations. When the amplitude of the dc triangle pulse was increased to  $\Phi_{LZS} > \Phi_r$ , striking interference fringes appeared. The positions of these interference fringes in the  $\Phi_{LZS} - t_\Lambda$  plane were nearly independent of the microwave power (Fig. 2b and 2c) but dependent on the microwave frequency (Fig. 2d). When  $\omega$  decreased,  $\Phi_r$  moved closer to  $\Phi_i$  as expected according to the measured spectrum shown in Fig. 1c. The resulting LZS interference fringes also moved closer to  $\Phi_i$ .

Using the dressed states picture, we can readily capture the underlying physics and provide a quantitative description of the observed interference patterns. The Hamiltonian of the microwave-

dressed qubit can be written as:

$$H_0 = H_q(t) + H_m + H_{q-m}. \quad (1)$$

In Eq. (1),  $H_q(t) = \frac{1}{2}\omega_{10}(t)\sigma_z^q$  is the Hamiltonian of the qubit, where  $\sigma_z^q$  is Pauli Z operator on the qubit and  $\omega_{10}(t)$  is the energy level spacing of the bare qubit, which can be controlled *in situ* by the dc triangular pulse. The Hamiltonian of the microwave field is  $H_m = \omega a^\dagger a$ , where  $a^\dagger$  and  $a$  are the creation and annihilation operators, respectively. The interaction Hamiltonian then is  $H_{q-m} = g(a^\dagger\sigma_-^q + a\sigma_+^q)$ , where  $g$  is the coupling strength between the microwave field and the qubit,  $\sigma_-^q$  and  $\sigma_+^q$  are the raising and lowering operators on the qubit. Truncating  $H_0$  in the subspace spanned by  $\{|1, n\rangle, |0, n+1\rangle\}$ , where  $|n\rangle$  is the Fock state of the microwave field, we obtain:

$$H_0 = \begin{pmatrix} \omega_{10}(t)/2 + n\omega & \Omega_R/2 \\ \Omega_R/2 & -\omega_{10}(t)/2 + (n+1)\omega \end{pmatrix}, \quad (2)$$

where the Rabi frequency  $\Omega_R = g\sqrt{n+1}$ .  $H_0$  can be transformed to:

$$H_0 = \begin{pmatrix} 0 & \Omega_R/2 \\ \Omega_R/2 & \delta(t) \end{pmatrix}, \quad (3)$$

where  $\delta(t) = \omega - \omega_{10}(t)$  is the detuning. The coupling between the two microwave dressed states  $|0, n+1\rangle$  and  $|1, n\rangle$  is analog to the tunnel splitting between the  $|\uparrow\rangle$  and  $|\downarrow\rangle$  states of a spin in the presence of a weak transverse magnetic field. The LZS interference occurs when the dc triangle pulse sweeps back and forth across this avoided crossing whose minimum gap is  $\Omega_R$ . When the microwave power increases,  $\Omega_R$  increases, which subsequently affects the detailed structures but has negligible effect on the positions of the fringes, as shown in Fig. 2g. Here the one-dimensional

data are extracted from Fig. 2a, 2b and 2c at  $\Phi_{LZS} = 5 \text{ m}\Phi_0$ . The maximum height of the interference peaks was reached earlier with the stronger microwave field. This observation agrees with our intuitive expectation because a stronger microwave field leads to a larger splitting, thereby the phase difference accumulates at a faster rate.

Another interesting phenomenon is the relationship between the peak height ( $h$ ) and  $\Omega_R$  for different microwave powers. Shown in Fig. 2g are examples of  $P_1$  versus  $t_\Lambda$  at three microwave powers, with coupling strength  $\Omega_{Ra}/2\pi = 19.6 \text{ MHz}$  (green circles),  $\Omega_{Rb}/2\pi = 27.8 \text{ MHz}$  (red circles) and  $\Omega_{Rc}/2\pi = 41.7 \text{ MHz}$  (blue circles), respectively. Almost three periods of oscillations were observed in all cases. It is noticed that in the first period one has  $h(\Omega_{Ra}) > h(\Omega_{Rb}) > h(\Omega_{Rc})$ , while in the second and the third periods the order changes to  $h(\Omega_{Rb}) > h(\Omega_{Rc}) > h(\Omega_{Ra})$  and  $h(\Omega_{Rc}) > h(\Omega_{Rb}) > h(\Omega_{Ra})$ , respectively. As discussed below the observed reversal in the order of the relative peak strengths is also the result of LZS interference between the microwave dressed qubit states.

As shown in the previous work<sup>15</sup>, the LZ transition rate  $P_T$  from  $|0\rangle$  to  $|1\rangle$  is approximately given by  $P_T = 4P_{LZ}(1 - P_{LZ})$  with  $P_{LZ} = \exp(-\eta)$ , where  $\eta \equiv 2\pi(\Omega_i/2)^2/\nu$ ,  $\Omega_i$  ( $i = Ra, Rb, Rc$ ) is the minimum gap of the avoided crossing, and  $\nu$  denotes the rate of the changing energy level spacing of the noninteracting levels. The solid lines in the insets of Fig. 2g show the dependence of  $P_T$  on  $\eta$ . Then we calculated  $\eta$  and  $P_T$  for the maximum value in each of the three periods and marked them with color dots on  $P_T(\eta)$ . The relationship of  $P_T$  at different powers agree with the observed one. Therefore, although the relative strength of the peaks seems

random due to extrinsic fluctuations, it is actually a manifestation of the physical laws that govern the dynamics of the interacting qubit-microwave field system. Furthermore, this result indicates that by adjusting the microwave power and the sweep rate of the dc triangle pulse, one can control the qubit states coherently. In addition, one can also control  $\delta(t)$ , thus shift the positions of the fringes, by varying the frequency of the microwave.

Though the LZS interference has been used mostly to characterize the parameters defining the quantum systems and their interaction with the environment, recent works suggest that it has great potential in the coherent manipulation of quantum states, in particular multipartite quantum states<sup>15,16</sup>. In this context, the existence of avoided crossings in the energy diagram of single qubit or coupled multiple qubits<sup>15</sup> are crucial to produce the LZS interference. The disadvantage of such intrinsic avoided crossings is that it is usually difficult to control the location and the gap size *in situ* once the qubits are fabricated. A more fundamental problem is that for certain types of qubits such as the SPQ, the computational basis states do not have intrinsic avoided crossings. But in the LZS interference of the microwave dressed states, one can create and/or adjust the position and gap size of the avoided crossings as one desires. This method is particularly advantageous in manipulating the states of multi-qubit systems as discussed below.

Let's consider the case of a TLS coupled to the SPQ. Note that when the tip of the dc triangle pulse reached the center of the qubit-TLS1 avoided crossing  $\Phi_{TLS1}$ , another group of interference fringes emerged (Fig. 2a). These additional LZS interference fringes were the results of the coupling between the qubit and TLS1. In fact, the fringes in Fig. 2a were similar to those observed

in the previous work<sup>15</sup>. Taking into account the existence of TLS1, the Hamiltonian of the entire qubit-TLS-microwave field system becomes  $H_1 = H_0 + H_{T_1} + H_{q-T_1}$ . The Hamiltonian of TLS1 is  $H_{T_1} = \frac{1}{2}\omega_{T_1}\sigma_z^{T_1}$ , where  $\omega_{T_1}$  is the energy level spacing of TLS1 and  $\sigma_z^{T_1}$  is Pauli Z operator on the TLS1. The interaction Hamiltonian is  $H_{q-T_1} = g_1\sigma_x^q \otimes \sigma_x^{T_1}$ , where  $g_1$  is the coupling strength between the qubit and TLS1,  $\sigma_x^q$  and  $\sigma_x^{T_1}$  are Pauli X operators on the qubit and TLS1, respectively. In the subspace spanned by  $\{|1g, n\rangle, |0g, n+1\rangle, |0e, n\rangle\}$ ,  $H_1$  can be simplified as:

$$H_1 = \begin{pmatrix} 0 & \Omega_R/2 & g_1 \\ \Omega_R/2 & \delta(t) & 0 \\ g_1 & 0 & \delta_1(t) \end{pmatrix}, \quad (4)$$

where  $\delta_1(t) = \omega_{T_1} - \omega_{10}(t)$ . To facilitate quantitative comparisons between the theory and experiment, we averaged over different values of  $n$  assuming the microwave field is in a coherent state<sup>10</sup> characterized by  $\langle n \rangle$  and solved the corresponding Bloch equation numerically. The results agree quantitatively with the experimental data, as shown in Fig. 2e and Fig. 2f. The overall good agreement confirms the validity of our understanding and treatment of the multipartite system interacting with the microwave field.

Another parameter that could dramatically affect the LZS interference of the microwave dressed states of the SPQ is the initial state of the qubit. Of special interest is when the qubit was initially biased at the point where the microwave was resonant with  $\omega_{10}$ , i.e.,  $\Phi_i = \Phi_r$ . In this case, we set  $t_{mw} \geq t_\Lambda$  as shown with dotted line in Fig. 1b and found that the difference between them,  $t_i = t_{mw} - t_\Lambda$ , affected the interference fringes significantly. We measured the LZS interference for  $t_i = 0, 7 \text{ ns}, 13 \text{ ns}, 19 \text{ ns}$  and  $750 \text{ ns}$ , corresponding to the  $0, \pi/2$  pulse,  $\pi$  pulse,  $3\pi/2$  pulse



and mixed states in Rabi oscillation with  $\omega/2\pi = 16.345$  GHz and the nominal power 13 dBm, respectively. As shown in Fig. 3a-3e, the interference fringes are very sensitive to  $t_i$ , because different  $t_i$  results in different initial states of the qubit at the beginning of the dc triangle pulse, i.e., different probability amplitudes of  $|0\rangle$  and  $|1\rangle$ . The corresponding numerical results are shown in Fig. 3f-3j. It is noticed that in Fig. 3a, both  $\Phi_{LZS} \geq \Phi_i$  and  $\Phi_{LZS} < \Phi_i$  are included. Thus three microscopic TLSs (TLS1, TLS2, and TLS3) were involved into the evolution as shown in Fig. 1b and Fig. 1c. The qubit and the three TLSs now form a tetrapartite quantum system, the Hamiltonian of which is  $H_2 = H_0 + \sum_{i=1}^3 \frac{1}{2} \omega_{T_i} \sigma_z^{T_i} + \sum_{i=1}^3 g_i \sigma_x^q \otimes \sigma_x^{T_i}$ . In the subspace spanned by  $\{|1g_1g_2g_3, n\rangle, |0g_1g_2g_3, n+1\rangle, |0e_1g_2g_3, n\rangle, |0g_1e_2g_3, n\rangle, |0g_1g_2e_3, n\rangle\}$ ,  $H_2$  can be written as:

$$H_2 = \begin{pmatrix} 0 & \Omega_R/2 & g_1 & g_2 & g_3 \\ \Omega_R/2 & \delta(t) & 0 & 0 & 0 \\ g_1 & 0 & \delta_1(t) & 0 & 0 \\ g_2 & 0 & 0 & \delta_2(t) & 0 \\ g_3 & 0 & 0 & 0 & \delta_3(t) \end{pmatrix}, \quad (5)$$

where  $\delta_i(t) = \omega_{TLSi} - \omega_{10}(t)$ , and  $g_i$  is the coupling strength between the qubit and the  $i$ th TLS ( $i=1, 2, 3$ ). From Fig. 3 one can see that the agreement between the numerical simulation and experimental results is quite remarkable. This further confirms that the LZS interference can be a powerful tool for controlling multi-partite quantum systems. It should be pointed out that the width of the triangle pulse is much shorter than the decoherence time. Therefore, the system's evolution remains coherent. To the best of our knowledge, this is the first demonstration of controlling tetrapartite coherent evolution in a solid-state quantum system.

We have previously shown that the intrinsic avoided crossings of a tripartite system can be used as quantum beam splitters<sup>15</sup> to construct quantum logic gates. The demonstration of LZS interference of the microwave dressed states enhance the efficiency and flexibility of this novel approach to multi-qubit quantum gates. Compared to the Stark-chirped rapid adiabatic passage (SCRAP) method<sup>24,25</sup>, the LZS interference based quantum gates achieve two significant improvements: (i) The qubit flux bias remains unchanged after the gate operations. This will significantly simplify the subsequent operations and increase the gate fidelity; (ii) The location and intensity of the LZS interference can be controlled *in situ* by adjusting the sweeping rate, the microwave power as well as frequency. It is thus very promising for quantum information applications such as the implementation of much faster multi-qubit quantum gates.

Our experiment has verified that the macroscopic artificial atom, SPQ, interacts with the microwave field the same way as atoms interact with light. The concept of dressed states not only provides an excellent intuitive picture to understand qualitatively the behavior of such complicated system but also a theoretical foundation for quantitative simulation and prediction of the system's dynamics. Moreover, it can also be generalized to other systems interacting with electromagnetic fields, opening a new route toward the realization of large scale quantum information processing.

**Figure 1** Qubit circuit, experimental procedure and spectrum. **a**, Schematic of the qubit circuitry. An rf-SQUID with an Al/AlOx/Al junction denoted by the X symbol serves as the SPQ. The inductance of the superconducting loop is about 770 pH. The capacitance and critical current of the junction are about 240 fF and 1.4  $\mu$ A, respectively. The flux bias, microwave and readout dc-SQUID are inductively coupled to the qubit. **b**, Schematic of measuring the LZS interference of the microwave dressed states of the SPQ. The two lowest eigenstates  $|0\rangle$  and  $|1\rangle$  form the qubit with the transition frequency  $\omega_{10}$  that can be rapidly adjusted *in situ* by changing the flux bias. A microwave pulse is used to create an avoided energy level crossing centered at  $\omega = \omega_{10}$ . The microwave dressed states are denoted by  $|0, n+1\rangle$  and  $|1, n\rangle$ . A dc triangle pulse (solid line for  $\Phi_i \neq \Phi_r$  and dotted line for  $\Phi_i = \Phi_r$ ) is applied to sweep the system through the avoided crossing of the dressed states. The avoided crossings caused by the qubit-TLS interaction are also shown with  $2g_1/2\pi = 60$  MHz,  $2g_2/2\pi = 22$  MHz and  $2g_3/2\pi = 46$  MHz, respectively. **c**, Measured spectroscopy of the SPQ. Three avoided crossings induced by the qubit-TLS interaction are observed. The inset shows a general avoided level crossing. The dashed and solid lines represent the energies of the uncoupled and coupled states, respectively.

**Figure 2** The LZS interference in the SPQ. **a, b, c**, The LZS interference with  $\omega/2\pi = 16.345$  GHz. The Rabi frequencies are  $\Omega_{Ra}/2\pi = 19.6$  MHz,  $\Omega_{Rb}/2\pi = 27.8$  MHz and  $\Omega_{Rc}/2\pi = 41.7$  MHz, respectively. **d**, The LZS interference with  $\omega/2\pi = 16.315$  GHz and Rabi frequency 30.9 MHz. The microwave frequency essentially determines the location of the interference fringes. Decreasing the microwave frequency results in a shift of the

interference fringes toward the initial flux bias. **e**, Numerically calculated LZS interference fringes using  $H_2$  with  $\omega/2\pi = 16.345$  GHz. The Rabi frequency is 19.6 MHz. **f**, The dependence of population of  $|1\rangle$  on  $t_\Lambda$  with  $\omega/2\pi = 16.345$  GHz at  $\Phi_{LZS} = 5 \text{ m}\Phi_0, 10 \text{ m}\Phi_0, 12 \text{ m}\Phi_0$ , respectively. The Rabi frequency is 19.6 MHz. The circles represent the experimental data and the lines are extracted from Fig. 2e. **g**, The dependence of population of  $|1\rangle$  on  $t_\Lambda$  (ns) at  $\Phi_{LZS} = 5 \text{ m}\Phi_0$  with  $\Omega_{Ra}/2\pi = 19.6$  MHz (green circles),  $\Omega_{Rb}/2\pi = 27.8$  MHz (red circles) and  $\Omega_{Rc}/2\pi = 41.7$  MHz (blue circles), respectively. Maxima are marked with color arrows. The insets show the positions of each maximum with color dots in  $P_T(\eta)$ , which illustrate the relationship between the heights of the maxima intuitively.

**Figure 3** Dependence of the LZS interference between the microwave dressed states on the initial state of the qubit as characterized by  $t_i$  (c.f. Fig. 1b). **a**,  $t_i=0$  corresponds to the initial state  $\Psi_i = |0\rangle$ . **b**,  $t_i=7$  ns, for  $\Psi_i = (|0\rangle - i|1\rangle)/\sqrt{2}$ . **c**,  $t_i=13$  ns, for  $\Psi_i = |1\rangle$ . **d**,  $t_i=19$  ns, for  $\Psi_i = (|0\rangle + i|1\rangle)/\sqrt{2}$ . **e**,  $t_i=750$  ns, for the mixed state  $\frac{1}{2}(|0\rangle\langle 0| + |1\rangle\langle 1|)$ . **f, g, h, i, j**, Numerically simulated LZS interference fringes for  $t_i=0, 7$  ns, 13 ns, 19 ns and 750 ns, respectively.

1. Cohen-Tannoudji, C., Dupont-Roc, J. & Grynberg, G. *Atom-Photon Interactions: basic processes and applications* (Wiley, New York, 1992).
2. Yang, C.-P., Chu, S.-I. & Han, S. Possible realization of entanglement, logical gates, and quantum-information transfer with superconducting-quantum-interference-device qubits in cavity qed. *Phys. Rev. A* **67**, 042311 (2003).
3. You, J. Q. & Nori, F. Quantum information processing with superconducting qubits in a microwave field. *Phys. Rev. B* **68**, 064509 (2003).
4. Schoelkopf, R. J. & Girvin, S. M. Wiring up quantum systems. *Nature* **451**, 664–669 (2008).
5. Shevchenko, S., Ashhab, S. & Nori, F. Landau-Zener-Stückelberg interferometry. *Physics Reports* **492**, 1–30 (2010).
6. Martinis, J. M. Superconducting phase qubits. *Quantum Inf. Process.* **8**, 81–103 (2009).
7. Yoakum, S., Sirko, L. & Koch, P. M. Stueckelberg oscillations in the multiphoton excitation of helium rydberg atoms: Observation with a pulse of coherent field and suppression by additive noise. *Phys. Rev. Lett.* **69**, 1919–1922 (1992).
8. Oliver, W. D. *et al.* Mach-Zehnder interferometry in a strongly driven superconducting qubit. *Science* **310**, 1653–1657 (2005).
9. Sillanpää, M., Lehtinen, T., Paila, A., Makhlin, Y. & Hakonen, P. Continuous-time monitoring of Landau-Zener interference in a cooper-pair box. *Phys. Rev. Lett.* **96**, 187002 (2006).

10. Wilson, C. M. *et al.* Coherence times of dressed states of a superconducting qubit under extreme driving. *Phys. Rev. Lett.* **98**, 257003 (2007).
11. Izmailkov, A. *et al.* Consistency of ground state and spectroscopic measurements on flux qubits. *Phys. Rev. Lett.* **101**, 017003 (2008).
12. Rudner, M. S. *et al.* Quantum phase tomography of a strongly driven qubit. *Phys. Rev. Lett.* **101**, 190502 (2008).
13. Sun, G. *et al.* Population inversion induced by Landau–Zener transition in a strongly driven rf superconducting quantum interference device. *Appl. Phys. Lett.* **94**, 102502 (2009).
14. LaHaye, M. D., Suh, J., Echternach, P. M., Schwab, K. C. & Roukes, M. L. Nanomechanical measurements of a superconducting qubit. *Nature* **459**, 960–964 (2009).
15. Sun, G. *et al.* Tunable quantum beam splitters for coherent manipulation of a solid-state tripartite qubit system. *Nature Communications* **1**, 51 (2010).
16. Petta, J. R., Lu, H. & Gossard, A. C. A coherent beam splitter for electronic spin states. *Science* **327**, 669–672 (2010).
17. Makhlin, Y., Schön, G. & Shnirman, A. Quantum-state engineering with Josephson-junction devices. *Rev. Mod. Phys.* **73**, 357–400 (2001).
18. You, J. & Nori, F. Superconducting circuits and quantum information. *Physics Today* **58**, 42–47 (2005).
19. Clarke, J. & Wilhelm, F. K. Superconducting quantum bits. *Nature* **453**, 1031–1042 (2008).

20. Wilson, C. M. *et al.* Dressed relaxation and dephasing in a strongly driven two-level system. *Phys. Rev. B* **81**, 024520 (2010).
21. Simmonds, R. W. *et al.* Coherent interactions between phase qubits, cavities, and TLS defects. *Quantum Inf. Process.* **8**, 117–131 (2009).
22. Neeley, M. *et al.* Process tomography of quantum memory in a Josephson-phase qubit coupled to a two-level state. *Nature Physics* **4**, 523–526 (2009).
23. Zagoskin, A. M., Ashhab, S., Johansson, J. R. & Nori, F. Quantum two-level systems in Josephson junctions as naturally formed qubits. *Phys. Rev. Lett.* **97**, 077001 (2006).
24. Loy, M. M. T. Observation of population inversion by optical adiabatic rapid passage. *Phys. Rev. Lett.* **32**, 814–817 (1974).
25. Wei, L. F., Johansson, J. R., Cen, L. X., Ashhab, S. & Nori, F. Controllable coherent population transfers in superconducting qubits for quantum computing. *Phys. Rev. Lett.* **100**, 113601 (2008).

**Acknowledgements** This work was supported in part by NCET, NSFC (11074114), the State Key Program for Basic Research of China (2011CB922104), and NSF Grant No. DMR-0325551. SH also acknowledges partial support from DMEA Contract No. H94003-04-D-0004-0149. We gratefully acknowledge Northrop Grumman ES in Baltimore MD for foundry support and thank R. Lewis, A. Pesetski, E. Folk, and J. Talvacchio for technical assistance.

**Competing Interests** The authors declare that they have no competing financial interests.

**Correspondence** Correspondence and requests for materials should be addressed to G.S. (email: gz-sun@nju.edu.cn) or S.H.(email: han@ku.edu).



[Fig1.]

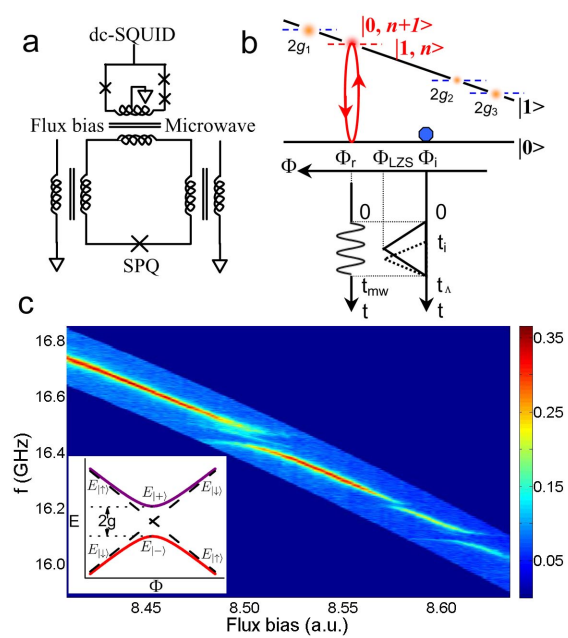


[Fig2.]

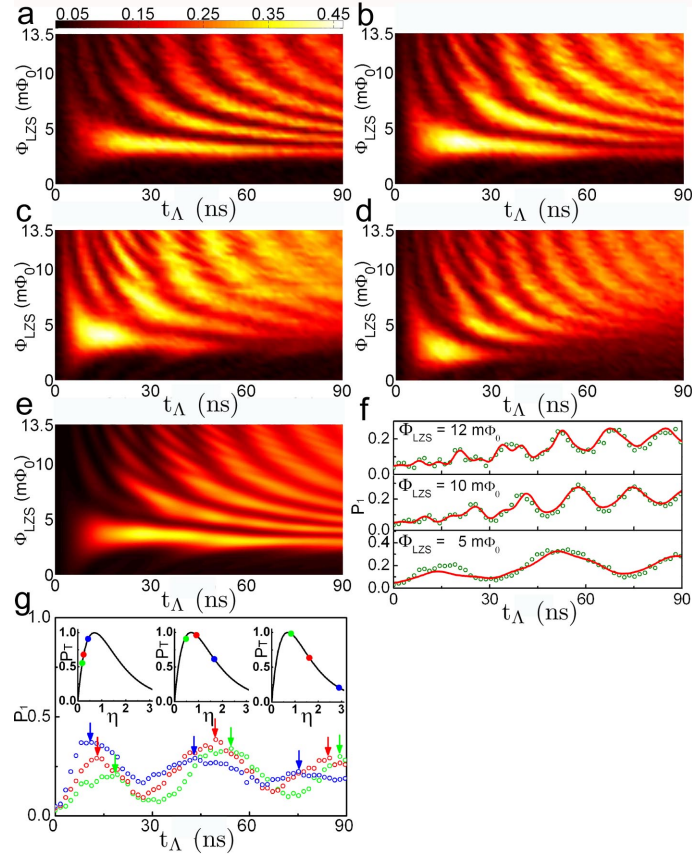


[Fig3.]

